Eur. Phys. J. A (2020) 56:127
https://doi.org/10.1140/epja/s10050-020-00145-5

THE EUROPEAN PHYSICAL JOURNAL A

Regular Article -Theoretical Physics

Yrast band in the heavy $N = Z$ nucleus ^{88}Ru: α-cluster approach

Peter Mohr[1,2,a]

[1] Institute for Nuclear Research (Atomki), 4001 Debrecen, Hungary
[2] Diakonie-Klinikum, 74523 Schwäbisch Hall, Germany

Received: 10 March 2020 / Accepted: 11 April 2020 / Published online: 18 May 2020

Communicated by Emiko Hiyama

Abstract The yrast band in the heavy $N = Z$ nucleus ^{88}Ru is studied in the framework of the α-cluster model in combination with double-folding potentials. It is found that the excitation energies of the yrast band in ^{88}Ru can be nicely described within the α-cluster approach using a smooth and mildly L-dependent adjustment of the potential strength. This result is similar to well-established α-cluster states in nuclei with a (magic core $\otimes\ \alpha$) structure. Contrary, the yrast bands in neighboring $N \neq Z$ nuclei deviate from such a typical α-cluster behavior. Finally, the α-cluster model predicts reduced transition strengths of about 10 Weisskopf units for intraband transitions between low-lying states in the yrast band of ^{88}Ru.

1 Introduction

The structure of the heaviest accessible $N = Z$ nuclei has been subject of interest over the last years, with one focus on the role of proton–neutron pairing [1,2]. Very recently, a detailed experimental investigation of ^{88}Ru became available which provided the excitation energies of the yrast band up to $J^\pi = (14^+)$ and $E^* = 6949$ keV [3]. It was concluded that the observed yrast band in ^{88}Ru exhibits a band crossing "that is significantly delayed compared with the expected bahavior of a rotating deformed nucleus in the presence of a normal isovector ($T = 1$) pairing field...in agreement with theoretical predictions for the presence of isoscalar neutron–proton pairing". But such an interpretation may also be affected by shape coexistence effects, and despite several detailed studies [3–7] a firm conclusion on the experimental verification of proton–neutron pairing could not yet be reached. The relevance of shape coexistence has also been pointed out in large-scale shell model calculations of heavy $N = Z$ nuclei [8].

In the present work I use a completely different approach for the description of the yrast band in ^{88}Ru which is based on the simple two-body α-cluster model. In general, α-clustering is a very well-known phenomenon in nuclear physics [9,10]. A lot of work has been done in the past for doubly-magic cores, i.e. ^{212}Po = ^{208}Pb $\otimes\ \alpha$, ^{44}Ti = ^{40}Ca $\otimes\ \alpha$, ^{20}Ne = ^{16}O $\otimes\ \alpha$, and ^{8}Be = ^{4}He $\otimes\ \alpha$ (see e.g. the recent review [9]), and ^{94}Mo = ^{90}Zr $\otimes\ \alpha$ was often used to fill the wide gap of missing stable doubly-magic core nuclei between $A \approx 40$ and $A > 200$ [11]. In this gap, the α-decay in the $N = Z$ system ^{104}Te = ^{100}Sn $\otimes\ \alpha$ was also under study very recently [12–16], and ^{52}Ti = ^{48}Ca $\otimes\ \alpha$ was investigated in [17]. A detailed introduction into the nuclear cluster model is provided in a dedicated special issue of [18–25].

In the last years, several successful attempts have been made to extend the α-cluster model towards semi-magic core nuclei (e.g., above $N = 50$ [26]), and α-cluster states have also been identified in non-magic ^{46,54}Cr [27,28]. Thus, it makes sense to apply the α-cluster model to ^{88}Ru to see whether the properties of ^{88}Ru can also be described without explicit inclusion of proton–neutron pairing. It has to be noted that the α-cluster model and proton–neutron pairing are not completely different approaches. It was already supposed in [5] that the collaboration of the usual proton–proton and neutron–neutron pairing with enhanced proton–neutron pairing in ^{88}Ru may lead to α-like correlations, but unfortunately this idea remained qualitative in [5] and was not detailed further.

The present study is organized as follows. Section 2 provides a brief introduction into the chosen model. Section 3 gives results for ^{88}Ru and some neighboring $N = Z$ and $N \neq Z$ nuclei. The results are summarized in Sect. 4. Experimental data are taken from the online database ENSDF [29], except stated explicitly in the text.

[a] e-mail: mohr@atomki.mta.hu (corresponding author)

2 α clustering and folding potentials

Details of the α-cluster model are described in literature (e.g., [18–25]). Exactly the same approach was used in my previous paper on ^{46,54}Cr [28]. Here I briefly repeat important features of the model and its essential ingredients.

2.1 Folding potential

The interaction between the α particle and the core nucleus is calculated from the folding procedure with the widely used energy- and density-dependent DDM3Y interaction $v_{\rm eff}$:

$$V_F(r) = \int\int \rho_P(r_P)\,\rho_T(r_T)\,v_{\rm eff}(s,\rho,E_{\rm NN})\,d^3r_P\,d^3r_T \tag{1}$$

For details of the folding approach and the chosen interaction $v_{\rm eff}$, see e.g. [35–37]. The density ρ_P of the α-particle is taken from the experimental charge density distribution [38]. Obviously, for ^{88}Ru = ^{84}Mo $\otimes$ α the required density of the unstable $N = Z$ nucleus ^{84}Mo is not available from experiment. It has been seen recently, that the usage of microscopic theoretical densities leads to very similar folding potentials [39]. In particular, Hartree–Fock–Bogolyubov densities using Skyrme forces were used in the present approach for all target densities ρ_T. These densities have been calculated by S. Goriely and are provided as a part of the statistical model code TALYS [40,41]. The folding integral in Eq. (1) was solved in the so-called "frozen-density" approximation.

The total interaction potential $V(r)$ is given by

$$V(r) = V_N(r) + V_C(r) = \lambda\,V_F(r) + V_C(r) \tag{2}$$

where the nuclear potential V_N is the double-folding potential V_F of Eq. (1) multiplied by a strength parameter $\lambda \approx 1.1 - 1.3$ [37,42]. V_C is the Coulomb potential in the usual form of a homogeneously charged sphere with the Coulomb radius R_C chosen the same as the root-mean-square radius $r_{\rm rms}$ of the folding potential V_F which approximately follows $r_{\rm rms} \approx R_0 \times A_T^{1/3}$ with $R_0 \approx 1.11 - 1.14$ fm for the nuclei under study. A_T (Z_T, N_T) will be used as the mass (charge, neutron) numbers of the "target" or core nucleus in the α-cluster model.

The strength parameter λ is adjusted to reproduce the energies of the bound states with $E < 0$ and quasi-bound states with $E > 0$ where $E = 0$ corresponds to the threshold of α emission in the compound nucleus. In general, $E = S_\alpha + E^*$ with the binding energy S_α of the α particle in the compound nucleus ($S_\alpha < 0$ for the nuclei under study) and the excitation energy E^*. The number of nodes N of the bound state wave function $u_{NL}(r)$ was derived from the Wildermuth condition

$$Q = 2N + L = \sum_{i=1}^{4}(2n_i + l_i) = \sum_{i=1}^{4} q_i \tag{3}$$

where Q is the number of oscillator quanta, N is the number of nodes, and L is the relative angular momentum of the α-core wave function. $q_i = 2n_i + l_i$ are the corresponding quantum numbers of the nucleons in the α cluster. Low-lying single-particle states around ^{88}Ru are dominated by the $g_{9/2}$ subshell, and thus I use $q_i = 4$, resulting in $Q = 16$. This leads to an yrast band with nine positive-parity states with J^π from 0^+ to 16^+ for the even-even nuclei under study.

Further details on the formalism for the calculations of the folding potentials $V_F(r)$, the resulting wave functions $u_{NL}(r)$, and reduced transition strengths $B(E\mathcal{L})$ have been provided in earlier work [15,26,42–44].

2.2 Evidence for α clustering

In light nuclei (e.g., ^{8}Be = ^{4}He $\otimes$ α or ^{20}Ne = ^{16}O $\otimes$ α) α-cluster states can be identified experimentally either by enhanced cross sections in α-transfer experiments like (^{6}Li,d) or by large reduced widths θ_α^2 in α-induced reactions. In heavy nuclei the preformation factor P in α-decay can provide valuable information on α-clustering of the decaying parent nuclei. However, for nuclei in the $A \approx 90$ mass region, the applicability of the above methods is limited. The lightest α emitters are found slightly above the doubly-magic core ^{100}Sn [14] which obviously excludes the $A \approx 90$ nuclei from α-decay studies. Compared to light nuclei, α-transfer studies like (^{6}Li,d) and the determination of reduced widths θ_α^2 are complicated for $A \approx 90$ nuclei by small cross sections because of the higher Coulomb barrier.

The well-established α-cluster states in light nuclei can be described as eigenstates in reasonably chosen α-nucleus potentials (like e.g. the double-folding potential). The resulting wave functions of these eigenstates can be used to calculate $E2$ transition strengths within α-cluster bands. In practice, these potentials show either a mild dependence on the angular momentum L (e.g., [43]), or very special radial shapes of the potential like the cosh potential [45] or combinations of Woods–Saxon plus cubed Woods–Saxon potentials with further modifications [27,46,47] have to be chosen. Note that a mild angular momentum dependence is expected for local effective potentials like the folding potential of the present study [48,49].

For nuclei in the $A \approx 90$ mass region, α-clustering is usually assumed as soon as the excitation energies E^* and $E2$ transition strengths for a rotational band can be described in the same way as explained for light nuclei in the previous paragraph [11,46]. Contrary, if the excitation energies of a band cannot be reproduced from reasonable α-nucleus potentials, theses states are not considered as α-cluster states.

For double-folding potentials, typically a smooth decrease of the potential strength parameter λ is found with increasing excitation energy or increasing angular momentum [26,43]. For intermediate mass nuclei around $N = 50$ an almost linear decrease of λ is found for the whole ground state band [26] whereas for the lightest nuclei the decreasing trend of λ may change to an increasing λ for states above $L \approx 6$ [43].

2.3 α-cluster properties of ^{96}Ru

Most previous studies (e.g., [11,46]) in the $A \approx 90$ mass region have focused on α-cluster states in ^{94}Mo = ^{90}Zr $\otimes$ α with the semi-magic $N_T = 50$ core ^{90}Zr. Experimentally, the 0^+ ground state and 2^+ first excited state in ^{94}Mo were populated in the ^{90}Zr(^{6}Li,d)^{94}Mo reaction [50], thus confirming the α-cluster properties of ^{94}Mo. Based on a theoretical study, it has been pointed out in [47] that several nuclei with a $(N_T = 50) \otimes \alpha$ structure show pronounced and very similar α-clustering properties. Besides ^{94}Mo, α-clustering is suggested for ^{90}Sr, ^{92}Zr, ^{96}Ru, and ^{98}Pd in [47]. In particular, this finding has been confirmed recently for ^{96}Ru by an α-transfer experiment using the ^{92}Mo(^{32}S,^{28}Si)^{96}Ru reaction where the ground state band and few states of a low-lying negative-parity band in ^{96}Ru were preferentially populated [51].

Based on the above theoretical and experimental arguments, the nucleus ^{96}Ru will be used as a reference for α-clustering in the following. ^{96}Ru is preferred over ^{94}Mo because the yrast band is completely identified up to $J^\pi = 16^+$ for ^{96}Ru whereas for ^{94}Mo levels are known only up to $J^\pi = (12^+)$. Note also that previous studies of ^{94}Mo were restricted up to $J^\pi = 10^+$ [46] and $J^\pi = 8^+$ [11], and both studies [11,46] disagreed on the location of the $J^\pi = 8^+$ state in ^{94}Mo.

3 Results and discussion

3.1 $N = Z$ nucleus ^{88}Ru = ^{84}Mo $\otimes$ α and some general remarks

Results for the potential strength parameter λ of ^{88}Ru are shown in Fig. 1; numerical values are summarized in Table 1. The obtained potential strength parameters λ show a mild, very smooth, and almost linear decrease from about $\lambda_0 \approx 1.27$ for the 0^+ ground state down to about 1.22 for the 14^+ state at $E^* = 6949$ keV.

For a perfect reproduction of $\lambda(L)$, a 4^{th}-order fit has been made (shown as dotted lines in Fig. 1):

$$\lambda(L) = \lambda_0 \times \left[1 + \sum_{i=1}^{4} c_i L^i\right] \quad (4)$$

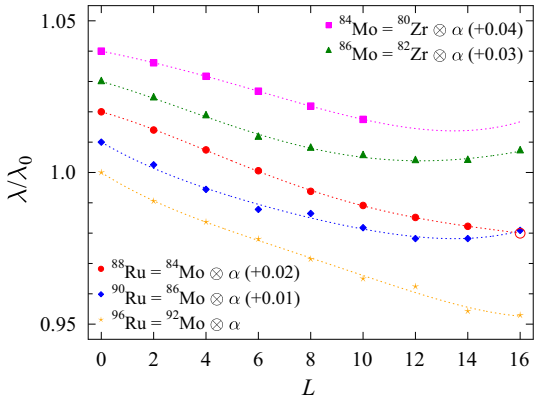

Fig. 1 Potential strength parameter λ (normalized to λ_0 for the $L = 0$ ground states) for ^{88}Ru = ^{84}Mo $\otimes$ α in comparison to the neighboring nuclei ^{84}Mo = ^{80}Zr $\otimes$ α, ^{86}Mo = ^{82}Zr $\otimes$ α, ^{90}Ru = ^{86}Mo $\otimes$ α, and ^{96}Ru = ^{92}Mo $\otimes$ α. The red open circle shows the prediction for the experimentally unknown $J^\pi = 16^+$ state in ^{88}Ru from Eq. (4) (see also Table 1). For better visibility, the results for the different nuclei are shifted by vertical offsets (0.01 per nucleus). Further discussion see text

Equation (4) provides an excellent description of $\lambda(L)$ for all nuclei under investigation in the present work and has thus been used in all cases.

Using Eq. (4), it is possible to extrapolate the experimentally based potential strength parameters λ of the 0^+ to 14^+ states to the unobserved $J^\pi = 16^+$ state, leading to $\lambda(16^+) = 1.2156$ which corresponds to an excitation energy of $E^*(16^+) \approx 8370$ keV.

It is interesting to note that the resulting volume integral J_R of the potential remains close to the recent ATOMKI-V1 global α-nucleus potential which was derived from elastic (α,α) scattering for heavy target nuclei at low energies around the Coulomb barrier [37]. This potential has also turned out to be very successful in the prediction of α-induced reaction cross sections at astrophysically relevant sub-Coulomb energies [39].

Finally, an intrinsic uncertainty for the derived potential strength parameters λ has to be briefly mentioned; fortunately, the relevance will turn out to be minor. The parameter λ_0 for the 0^+ ground states depends on the binding energy of the α-particle in the compound nucleus. Using the latest mass tables [52,53], the uncertainties of the α binding energies may reach up to almost 500 keV for the unstable $N = Z$ nuclei under study. Obviously, a larger binding energy is related to a larger λ value. However, a shift in energy by 500 keV corresponds only to a marginal change in λ of about 7×10^{-3}. This minor uncertainty affects all $\lambda(L)$ in the same direction and practically cancels out in the presentation and interpretation of λ/λ_0 in Fig. 1. For completeness, the α-binding energies S_α and the corresponding λ_0 are listed in Table 2 for all nuclei under investigation in the present study.

Table 1 α-cluster properties of ^{88}Ru. Experimental excitation energies are taken from [3]. Further discusssion see text

J^π	E^* (keV)	N	L	λ	J_R (MeV fm^3)	$B(E2, L \to L-2)$ (e^2 fm^4)	(W.u.)	Γ_γ (μeV)
0^+	0	8	0	1.2663	352.4	–	–	–
2^+	616	7	2	1.2587	350.2	203.7	8.8	15
4^+	1416	6	4	1.2504	347.9	281.2	12.1	76
6^+	2380	5	6	1.2417	345.5	285.2	12.3	196
8^+	3480	4	8	1.2331	343.1	260.3	11.2	346
10^+	4543	3	10	1.2272	341.5			
12^+	5696	2	12	1.2222	340.1			
14^+	6949	1	14	1.2185	339.1			
16^+ [a]	8370	0	16	1.2156	338.2			

[a]Results for 16^+ derived from the extrapolated $\lambda = 1.2156$ (see also Fig. 1)

Table 2 α-binding energies S_α from [52,53] and the resulting potential strength parameters λ_0 and volume integrals J_R of the 0^+ ground states

Nucleus	Z	N	core	Z_T	N_T	S_α (MeV)	λ_0	J_R (MeV fm^3)
^{84}Mo	42	42	^{80}Zr	40	40	−2.235	1.2800	357.6
^{86}Mo	42	44	^{82}Zr	40	42	−2.904	1.2716	354.1
^{88}Ru	44	44	^{84}Mo	42	42	−2.594	1.2663	352.4
^{90}Ru	44	46	^{86}Mo	42	44	−3.198	1.2583	348.9
^{96}Ru	44	52	^{92}Mo	42	50	−1.697	1.1942	327.7

In the following, the results for the $N = Z$ nucleus ^{88}Ru will be compared to ^{96}Ru with its neutron-magic ($N_T = 50$) core ^{92}Mo (Sect. 3.2), to all neighboring $N \neq Z$ nuclei with $N \pm 2$ or $Z \pm 2$ (Sects. 3.3, 3.4, and 3.5), and to the lighter $N = Z$ nucleus ^{84}Mo (Sect. 3.6).

3.2 Nucleus ^{96}Ru = ^{92}Mo $\otimes$ α with neutron-magic core ($N_T = 50$)

As a first comparison, we discuss the potential strength parameters $\lambda(L)$ for ^{96}Ru which is—besides ^{94}Mo [11,46] – a well-established α-cluster nucleus with a $N_T = 50$ neutron-magic core in this mass region. ^{96}Ru is preferred here because the yrast band is well-defined up to at least $J^\pi = 16^+$ whereas no high-spin members of the yrast band are available for ^{94}Mo (see also Sect. 2.3).

The calculations for ^{96}Ru in [26] have been repeated to ensure that the results are not affected by the present choice of the nucleon density of ^{92}Mo (see also Sect. 2.1). In both cases, using either an average density in [26] or using the theoretical density from [40,41] in the present study, it is found that the potential strength parameter λ depends only mildly and almost linear on the angular momentum L. Such a finding is typically interpreted as clear evidence for α-clustering. Interestingly, the L dependence of λ is very similar for ^{96}Ru and ^{88}Ru, pointing also to a significant amount of α-clustering in the $N = Z$ nucleus ^{88}Ru without magic core. Furthermore, a practically identical behavior was found for ^{98}Pd = ^{94}Ru $\otimes$ α, again with a neutron-magic core $N_T = 50$ [26].

3.3 Neighboring $N = Z + 2$ nucleus ^{90}Ru = ^{86}Mo $\otimes$ α

Contrary to ^{88}Ru and to the nuclei ^{96}Ru and ^{98}Pd with their neutron-magic $N_T = 50$ cores which all show an almost linear decrease of the potential strength parameter $\lambda(L)$, the $N \neq Z$ nucleus ^{90}Ru shows a clearly different behavior. The obtained values for λ show a somewhat larger scatter, and the trend of decreasing $\lambda(L)$ changes to increasing $\lambda(L)$ for the largest $L = 14$ and 16. Interestingly, a similar trend for $\lambda(L)$ is also found for an odd-parity band in ^{90}Ru which can be interpreted with $Q = 17$ in Eq. (3).

Both effects, a significantly larger scatter in $\lambda(L)$ and a non-monotonic bahavior, are usually interpreted that the simple α-cluster model is less applicable for such cases. Such a finding is not very surprising for ^{90}Ru which is a nucleus without a neutron-magic core.

3.4 Neighboring $N = Z + 2$ nucleus ^{86}Mo = ^{82}Zr $\otimes$ α

The results for the $N \neq Z$ nucleus ^{86}Mo are practically identical to the above results for ^{90}Ru. In particular, there is also a clear trend of increasing $\lambda(L)$ for the largest L under study. The scatter of the $\lambda(L)$ values is somewhat smaller

than for ^{90}Ru, but still above the very smooth results for ^{88}Ru and ^{96}Ru.

Similar to ^{90}Ru, also the $Q = 17$ odd-parity band in ^{86}Mo shows a trend of increasing $\lambda(L)$ for the largest L. However, because the $L = 15$ and $L = 17$ members are not known experimentally, the trend to increasing $\lambda(L)$ for large L is not as clear for ^{86}Mo as for ^{90}Ru.

3.5 Neighboring $N = Z - 2$ nuclei ^{86}Ru = ^{82}Mo $\otimes$ α and ^{90}Pd = ^{86}Ru $\otimes$ α

Unfortunately, the experimental information on these extremely neutron-deficient $N = Z - 2$ nuclei is very limited [29] because experiments with these neutron-deficient species are very difficult. In particular, it was not possible up to now to determine properties of rotational bands in these nuclei. Thus, although highly desirable, it is not possible to analyze the $N = Z - 2$ nuclei ^{90}Pd and ^{86}Ru in the same way as their $N = Z + 2$ mirror nuclei ^{90}Ru (Sect. 3.3) and ^{86}Mo (Sect. 3.4).

3.6 Neighboring $N = Z$ nucleus ^{84}Mo = ^{80}Zr $\otimes$ α

At first view, the resulting potential strength parameters $\lambda(L)$ for the $N = Z$ nucleus ^{84}Mo look very similar to the above results for ^{88}Ru. However, the observed yrast band in ^{84}Mo is known only up to $J^{\pi} = (10^{+})$ [6,29] which does not allow a strong statement on the behavior of $\lambda(L)$ for large angular momenta L. The 4^{th}-order fit in Eq. (4) shows a trend to increasing $\lambda(L)$ for large L, similar to the $N \neq Z$ nuclei ^{86}Mo and ^{90}Ru, but different from the neighboring $N = Z$ nucleus ^{88}Ru. A complete determination of the yrast band in ^{84}Mo up to $J^{\pi} = 16^{+}$ would be very important to answer the open question whether ^{84}Mo behaves really similar to its $N = Z$ neighbor ^{88}Ru.

Unfortunately, experimental data are also very limited for the next $N = Z$ nucleus ^{92}Pd, but very recently new data became available for ^{96}Cd [54]. Interestingly, the resulting $\lambda(L)$ for the $N = Z$ nucleus ^{96}Cd also show a clear trend of increasing $\lambda(L)$ for larger angular momenta L, i.e., similar to the $N \neq Z$ nuclei ^{86}Mo and ^{90}Ru, but different to the $N = Z$ nucleus ^{88}Ru.

3.7 Comparison and interpretation of the results

From the above results it is obvious that the yrast band in the $N = Z$ nucleus ^{88}Ru can be nicely described within the α-cluster model. Similar to well-established α-cluster nuclei like ^{96}Ru, the resulting potential strength parameters $\lambda(L)$ behave very regularly and show a smooth and almost linear trend to decrease towards larger angular momenta L. Contrary to the $N = Z$ nucleus ^{88}Ru, the neighboring $N \neq Z$ nuclei ^{86}Mo and ^{90}Ru show a different behavior with increasing $\lambda(L)$ towards large L. Interestingly, such a behavior is also found for the heavy $N = Z$ nucleus ^{96}Cd, and no clear conclusion is possible for the neighboring $N = Z$ nucleus ^{84}Mo. Also lighter $N \neq Z$ nuclei like ^{46}Cr and ^{54}Cr [28] show the typical $N \neq Z$ behavior of increasing $\lambda(L)$ for large L. Thus, the properties of the yrast band in ^{88}Ru seem to be somewhat extraordinary, and the interpretation of these data requires special care.

The different models for ^{88}Ru, i.e., α-clustering vs. proton–neutron pairing, can be further tested by comparing their predictions for reduced $E2$ transition strengths. The α-cluster model predicts $B(E2)$ of the order of 10 Weisskopf units for intraband transitions between low-lying members of the yrast band (see Table 1), and typically these predictions are in rough agreement with experiment even without the usage of effective charges and do not deviate by more than a factor of two from experimental values [26]. Contrary to the α-cluster model, various shell model approaches provide higher $E2$ strengths of 20 or even more Weisskopf units [5,8,55]. Very high values, even exceeding 50 Weisskopf units, were found from the consideration of proton–neutron pairing for the $B(E2, 8^{+} \rightarrow 6^{+})$, $B(E2, 6^{+} \rightarrow 4^{+})$, and $B(E2, 4^{+} \rightarrow 2^{+})$ transitions in the shell model [55] whereas the α-cluster model predicts almost constant $B(E2)$ for all transitions. Thus, a measurement of transition strengths could provide further insight in the applicability of the different models for ^{88}Ru. This holds in particular for transition strengths between excited states which are however extremely difficult to measure for ^{88}Ru. All present predictions of $B(E2)$ strengths from the shell model [5,8,55] and from the α-cluster model in this study lead to lifetimes far below nanoseconds in the yrast band and are thus compatible with the observation of γ-γ coincidences within the experimental nanosecond timing window of HPGe detectors [3].

4 Summary and conclusions

The α-cluster model is able to reproduce the excitation energies of the recently measured [3] yrast band in the heavy $N = Z$ nucleus ^{88}Ru. This provides an alternative approach to previous studies which had a focus on special proton–neutron pairing in $N = Z$ nuclei which was required to describe the observed delayed band crossing, compared to neighboring $N \neq Z$ nuclei. Both approaches—the α-cluster model on the one side and the shell model in combination with proton–neutron pairing on the other side—are able to reproduce the observed excitation energies of the yrast band in ^{88}Ru.

The experimental determination of radiation widths or absolute $E2$ transition strengths could be one way to test the reliability of the predictions from the different models and the applicability to ^{88}Ru. Without a clear experimentally

based preference for one of the models, any conclusion on the experimental verification of proton–neutron pairing in ^{88}Ru or on significant α-clustering in ^{88}Ru has to remain tentative.

Acknowledgements Open access funding provided by Institute for Nuclear Research. I thank Zs. Fülöp, Gy. Gyürky, G. G. Kiss, T. Szücs, and E. Somorjai for longstanding encouraging discussions on α-nucleus potentials. This work was supported by NKFIH (NN128072, K120666), and by the ÚNKP-19-4-DE-65 New National Excellence Program of the Ministry of Human Capacities of Hungary.

Data Availability Statement This manuscript has no associated data or the data will not be deposited. [Authors' comment: The manuscript has no associated data.]

References

1. S. Frauendorf, A.O. Macchiavelli, Prog. Part. Nucl. Phys. **78**, 24 (2014)
2. Y.H. Kim, M. Rejmund, P. Van Isacker, A. Lemasson, Phys. Rev. C **97**, 041302(R) (2018)
3. B. Cederwall et al., Phys. Rev. Lett. **124**, 062501 (2020)
4. X. Liu, S.Y. Xu, R. Fu, Sci. China **54**, 1811 (2011)
5. M. Hasegawa, K. Kaneko, T. Mizusaki, S. Tazaki, Phys. Rev. C **69**, 034324 (2004)
6. N. Marginean et al., Phys. Rev. C **65**, 051303(R) (2002)
7. S.M. Fischer et al., Phys. Rev. Lett. **87**, 132501 (2001)
8. A.P. Zuker, A. Poves, F. Nowacki, S.M. Lenzi, Phys. Rev. C **92**, 024320 (2015)
9. Z. Ren, B. Zhou, Front. Phys. **13**, 132110 (2018)
10. H. Horiuchi, K. Ikeda, K. Katō, Prog. Theor. Phys. Suppl. **192**, 1 (2012)
11. S. Ohkubo, Phys. Rev. Lett. **74**, 2176 (1995)
12. R.M. Clark, A.O. Macchiavelli, H.L. Crawford, P. Fallon, D. Rudolph, A. Såmark-Roth, M. Campbell, M. Cromaz, C. Morse, C. Santamaria, Phys. Rev. C **101**, 034313 (2020)
13. S. Yang, X. Chang, G. Röpke, P. Schuck, Z. Ren, Y. Funaki, H. Horiuchi, A. Tohsaki, T. Yamada, B. Zhou, Phys. Rev. C **101**, 024316 (2020)
14. K. Auranen et al., Phys. Rev. Lett. **121**, 182501 (2018)
15. P. Mohr, Europ. Phys. J. A **31**, 23 (2007)
16. X. Chang, Z. Ren, Phys. Rev. C **74**, 037302 (2006)
17. S. Ohkubo, Phys. Rev. C **101**, 041301(R) (2020)
18. S. Ohkubo, M. Fujiwara, P.E. Hodgson, Prog. Theor. Phys. Suppl. **132**, 1 (1998)
19. F. Michel, S. Ohkubo, G. Reidemeister, Prog. Theor. Phys. Suppl. **132**, 7 (1998)
20. T. Yamaya, K. Katori, M. Fujiwara, S. Kato, S. Ohkubo, Prog. Theor. Phys. Suppl. **132**, 73 (1998)
21. T. Sakuda, S. Ohkubo, Prog. Theor. Phys. Suppl. **132**, 103 (1998)
22. E. Uegaki, Prog. Theor. Phys. Suppl. **132**, 135 (1998)
23. M. Hasegawa, Prog. Theor. Phys. Suppl. **132**, 177 (1998)
24. S. Koh, Prog. Theor. Phys. Suppl. **132**, 197 (1998)
25. A. Tohsaki, Prog. Theor. Phys. Suppl. **132**, 213 (1998)
26. P. Mohr, The Open Nuclear and Particle Physics Journal **1**, 1 (2008). arXiv:0803.2202
27. M.A. Souza, H. Miyake, Europ. Phys. J. A **53**, 146 (2017)
28. P. Mohr, Europ. Phys. J. A **53**, 209 (2017)
29. Online database ENSDF, available at www.nndc.bnl.gov/ensdf; based on [30–34]
30. B. Singh, Nuclear Data Sheets **110**, 2815 (2009)
31. A. Negret, B. Singh, Nuclear Data Sheets **124**, 1 (2015)
32. E.A. McCutchan, A.A. Sonzogni, Nuclear Data Sheets **115**, 135 (2015)
33. E. Browne, Nuclear Data Sheets **82**, 379 (1997)
34. D. Abriola, A.A. Sonzogni, Nuclear Data Sheets **109**, 2501 (2008)
35. G.R. Satchler, W.G. Love, Phys. Rep. **55**, 183 (1979)
36. A.M. Kobos, B.A. Brown, R. Lindsay, G.R. Satchler, Nucl. Phys. A **425**, 205 (1984)
37. P. Mohr, G. G. Kiss, Zs. Fülöp, D. Galaviz, Gy. Gyürky, E. Somorjai, At. Data Nucl. Data Tables **99**, 651 (2013)
38. H. de Vries, C.W. de Jager, C. de Vries, Atomic Data and Nuclear Data Tables **36**, 495 (1987)
39. P. Mohr, Zs. Fülöp, Gy. Gyürky, G. G. Kiss, and T. Szücs, Phys. Rev. Lett., submitted
40. A.J. Koning, S. Hilaire, S. Goriely, computer code TALYS, version 1.8, http://www.talys.eu;
41. A.J. Koning, S. Hilaire, M.C. Duijvestijn, A.I.P. Conf, Proc. **769**, 1154 (2005)
42. U. Atzrott, P. Mohr, H. Abele, C. Hillenmayer, G. Staudt, Phys. Rev. C **53**, 1336 (1996)
43. H. Abele, G. Staudt, Phys. Rev. C **47**, 742 (1993)
44. F. Hoyler, P. Mohr, G. Staudt, Phys. Rev. C **50**, 2631 (1994)
45. B. Buck, A.C. Merchant, S.M. Perez, At. Data Nucl. Data Tables **54**, 53 (1993)
46. B. Buck, J.C. Johnston, A.C. Merchant, S.M. Perez, Phys. Rev. C **51**, 559 (1995)
47. M.A. Souza, H. Miyake, Phys. Rev. C **91**, 034320 (2015)
48. H. Horiuchi, Proc. *Int. Conf. on Clustering Aspects of Nuclear Structure and Nuclear Reactions*, Chester, UK, July 23–27, 1984, Eds. J. S. Lilley and M. A. Nagarajan, Springer Book https://www.springer.com/de/book/9789027720023
49. F. Michel, G. Reidemeister, Y. Kondō, Phys. Rev. C **51**, 3290 (1995)
50. H.W. Fulbright, C.L. Bennett, R.A. Lindgren, R.G. Markham, S.C. McGuire, G.C. Morrison, U. Strohbusch, J. Töke, Nucl. Phys. A **284**, 329 (1977)
51. U. Datta et al., AIP Conf. Proc. **2038**, 020020 (2018)
52. W.J. Huang, G. Audi, M. Wang, F.G. Kondev, S. Naimi, X. Xu, Chin. Phys. C **41**, 030002 (2017)
53. M. Wang, G. Audi, F.G. Kondev, W.J. Huang, S. Naimi, X. Xu, Chin. Phys. C **41**, 030003 (2017)
54. P.J. Davies et al., Phys. Rev. C **99**, 021302(R) (2019)
55. K. Kaneko, Y. Sun, G. de Angelis, Nucl. Phys. A **957**, 144 (2017)